

Local kinetic processes determining macroscopic properties of interlinked magnetic flux tubes

K.-J. Hwang¹, J. L. Burch¹, C. T. Russell², E. Choi¹, K. Dokgo¹, R. C. Fear³, S. A. Fuselier¹, S. M. Petrinec⁴, D. G. Sibeck⁵, H. Hasegawa⁶, H. Fu⁷, M. Øieroset⁸, C. P. Escoubet⁹, B. L. Giles⁵, R. J. Strangeway², Y. Khotyaintsev¹⁰, D. B. Graham¹⁰, D. J. Gershman⁵, C. J. Pollock¹¹, R. E. Ergun¹², R. B. Torbert¹³, and J. Broll¹⁴

¹ Southwest Research Institute, San Antonio, TX, USA

² Institute of Geophysics and Planetary Physics, University of California, Los Angeles, Los Angeles, CA, USA

³ University of Southampton, Southampton, UK

⁴ Lockheed Martin Advanced Technology Center, Palo Alto, CA 94304, USA

⁵ NASA Goddard Space Flight Center, Greenbelt, MD, USA

⁶ Institute of Space and Astronautical Science, Japan Aerospace Exploration Agency, Sagamihara, Japan

⁷ School of Science and Environment, Beihang University, Beijing, China

⁸ Space Sciences Laboratory, University of California, Berkeley, Berkeley, CA, USA

⁹ European Space Agency, the Netherlands

¹⁰ Swedish Institute of Space Physics, Uppsala, Sweden

¹¹ Denali Scientific, LLC, Fairbanks, AK, USA

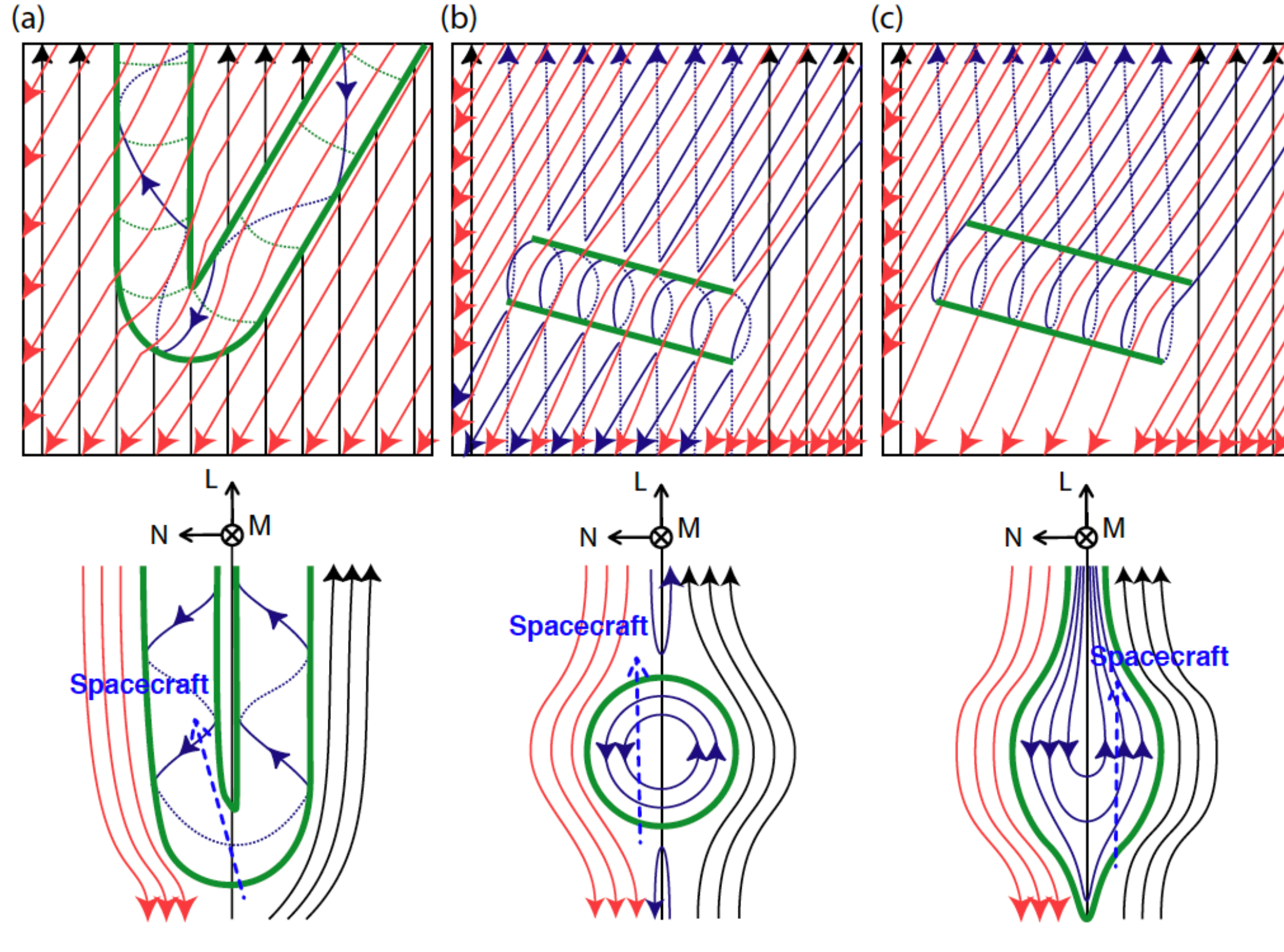
¹² Laboratory for Atmospheric and Space Physics, University of Colorado at Boulder, Boulder, CO, USA

¹³ Space Science Center, University of New Hampshire, Durham, NH, USA

¹⁴ Center for Space Physics, Boston University, Boston, MA, USA

Acknowledgements: MMS FPI, Fields, EPD, and Theory/Modeling teams

Formation models of flux transfer events (FTEs)



FTE models [Fear et al., 2008]:

- (a) Elbow-shaped FTE due to bursty reconnection (RX) [Russell and Elphic, 1978]
- (b) Multiple X-line model [Lee and Fu, 1985; Scholer, 1995]
- (c) Single X-line model [Scholer, 1988; Southwood et al., 1988; Phan et al., 2004]

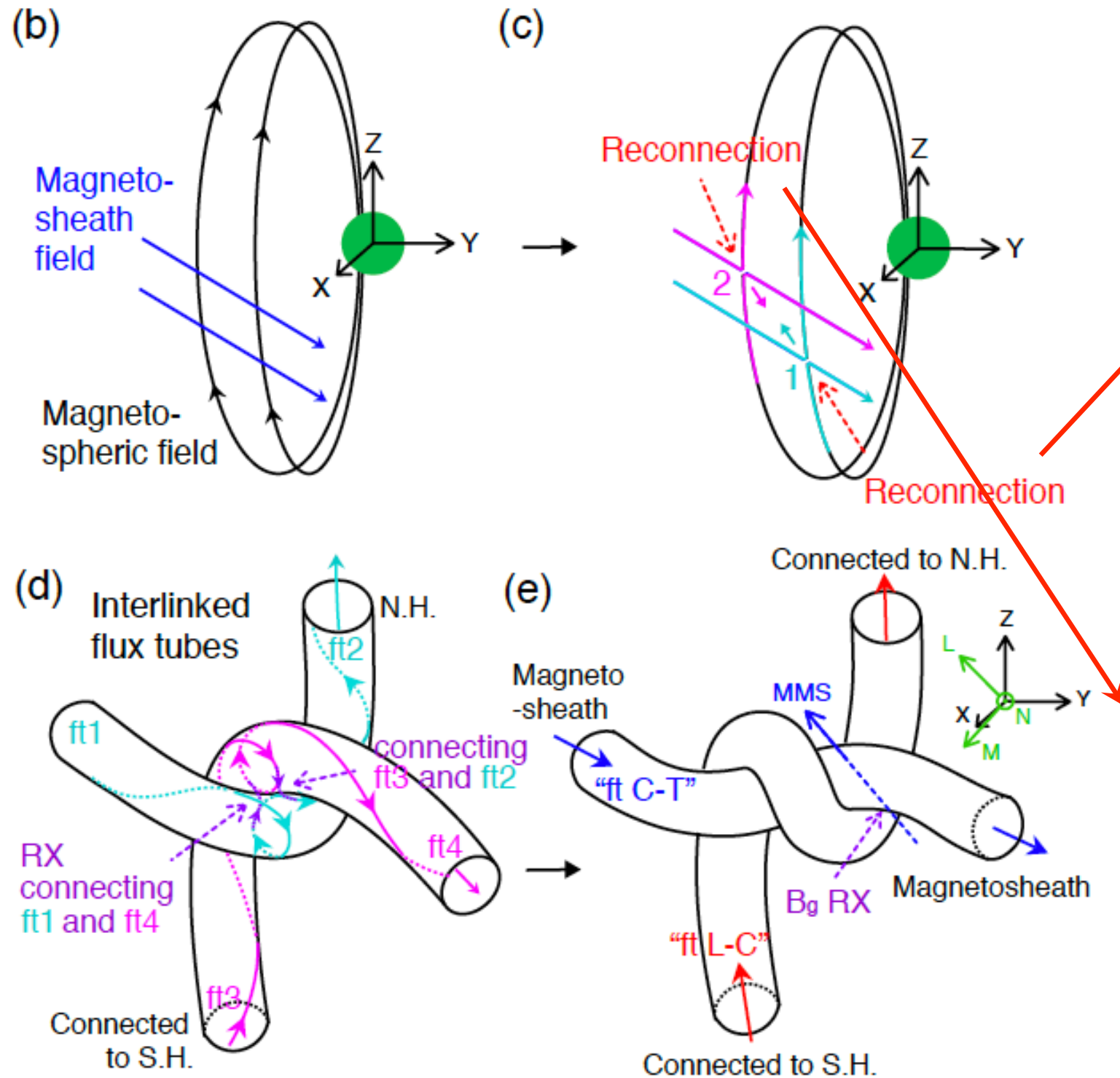
Common features:

- Bipolar Bn
- $|B|$ enhancement at the FTE center
- Mixture of Msphere and Msheath plasmas
- Invoke reconnection occurring around/at the edge of FTEs

New MMS observation:

- ⇒ A dip in $|B|$ at the FTE center
- ⇒ Msphere-only and Msheath-only regions within the FTE
- ⇒ Reconnection within/inside FTE or between two interlinked tubes might form a magnetic flux rope

Conclusion: generation of interlinked flux tubes with their connectivity to either both hemispheres or the magnetosheath [Hwang et al., 2020; under review]

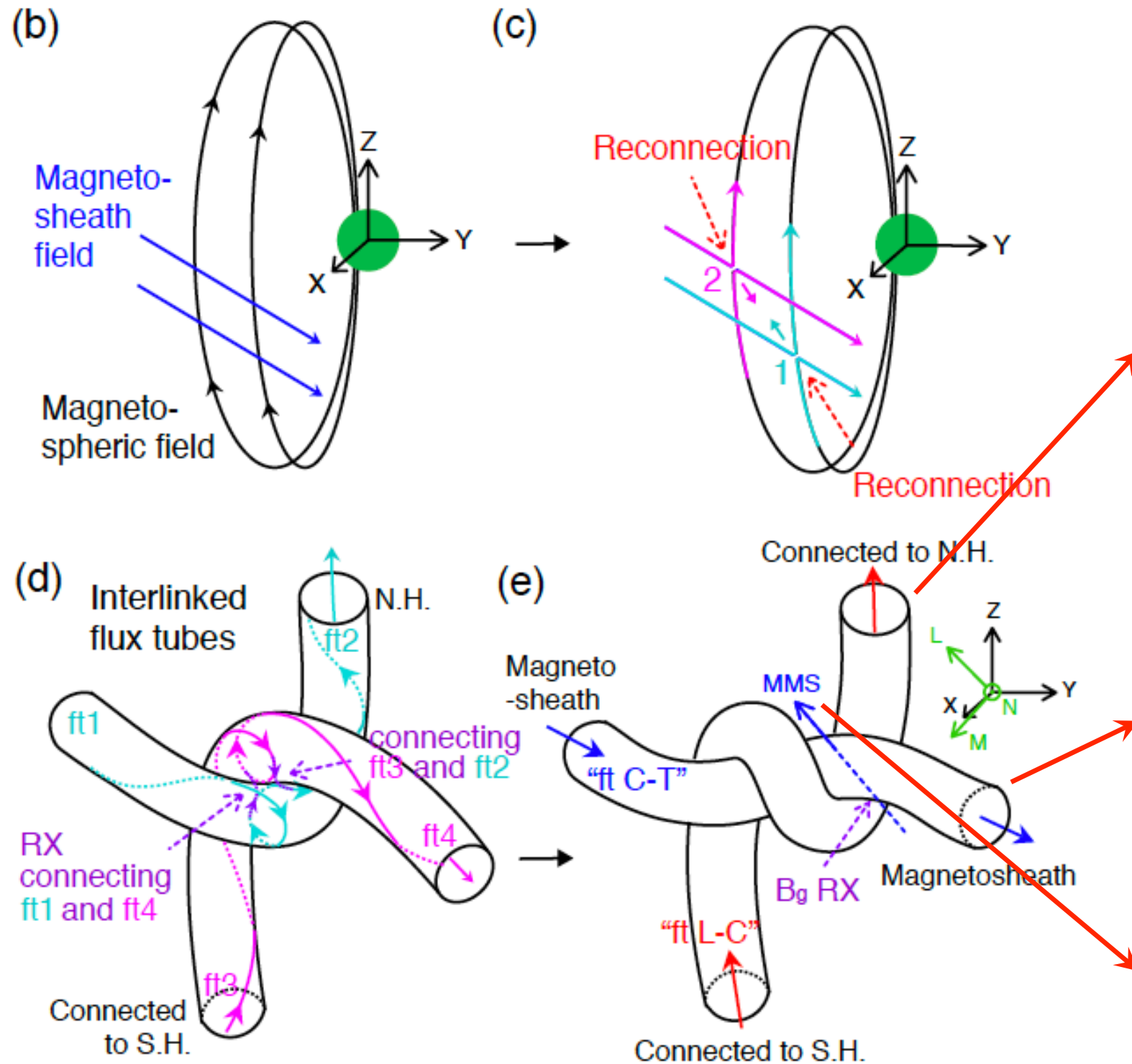


For the southward and duskward IMF (b):

Reconnected field lines at '1' in (c) (generating cyan field lines) can constitute a flux tube 'ft1'-'ft2' in (d), with one end connected to the northern hemisphere.

Reconnected field lines at '2' in (c) (generating magenta field lines) can constitute a flux tube 'ft3'-'ft4', with one end connected to the southern hemisphere (d).

Conclusion: generation of interlinked flux tubes with their connectivity to either both hemispheres or the magnetosheath [Hwang et al., 2020; under review]



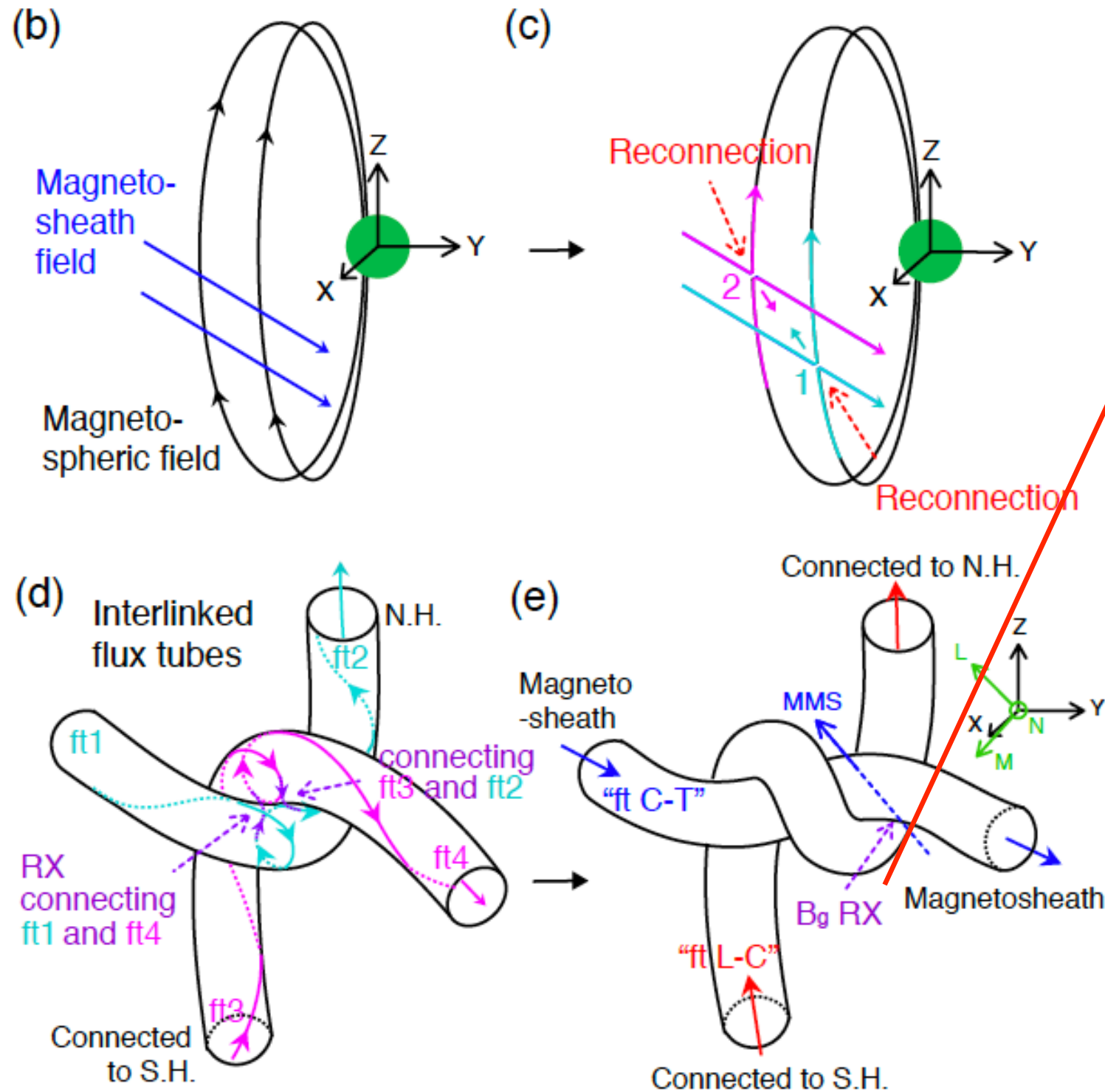
When the interface of the interlaced flux tubes undergoes reconnection (dashed violet arrows in d):

‘ft1’ and ‘ft4’ field lines are reconnected, constituting “ft C-T” with both ends connected to the magnetosheath (blue arrows in e).

‘ft2’ and ‘ft3’ field lines are reconnected, constituting “ft L-C” with both ends connected to the magnetosphere (red arrows in e).

MMS observed “ft L-C” first, then, “ft C-T”

Conclusion: generation of interlinked flux tubes with their connectivity to either both hemispheres or the magnetosheath [Hwang et al., 2020; under review]



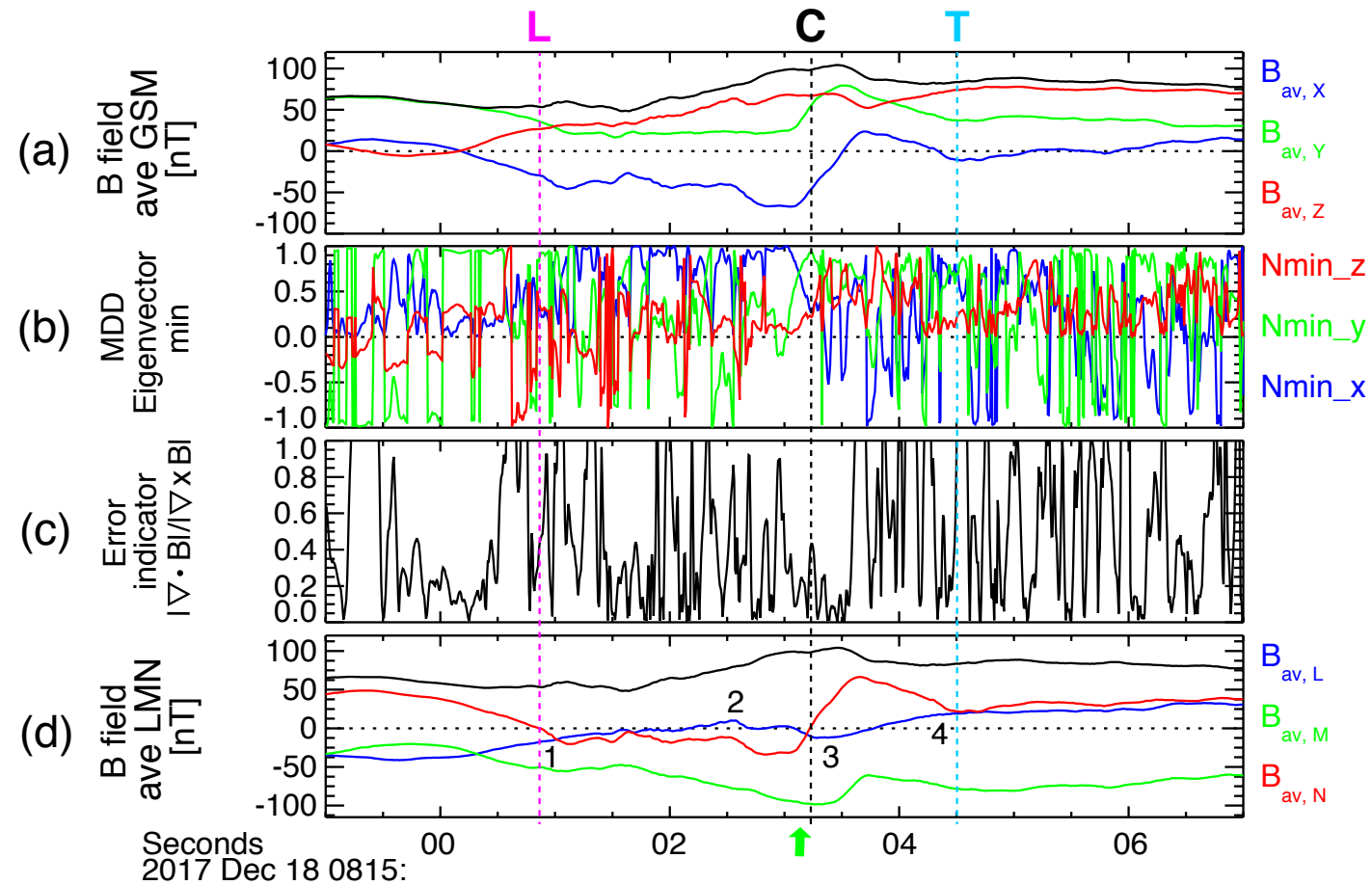
Reconnecting flux tubes (d) result in a more complicated structure (e).

This structure exerts strong magnetic tension force toward the interface of the two interlinked flux tubes, which facilitates an interaction, i.e., reconnection of the interface (dashed violet arrows in e).

Evidences from MMS observations:

- Perpendicular axes of two flux tubes
- Electron pitch angle distributions
- Reconnecting signatures at the interface.
- The magnetic curvature, $(\mathbf{B} \cdot \nabla \mathbf{B})_N / \mu_0$ showing a clear, bipolar reversal from + to - across the interface

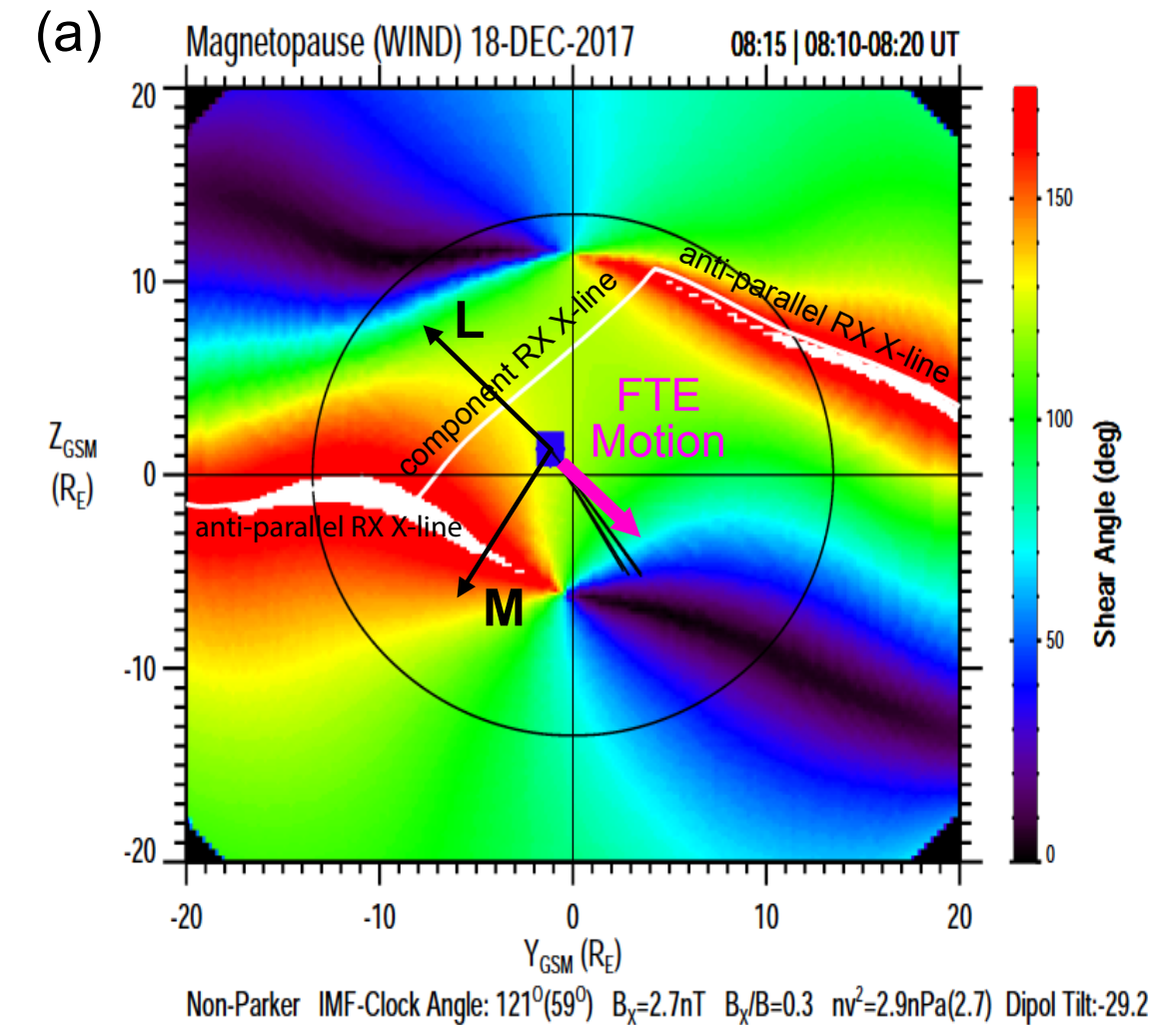
Overall orientation, motion, and scale size of an FTE



Using MVA and MDD, $\mathbf{L} = [0.39, -0.61, 0.69]$, $\mathbf{M} = [0.45, -0.52, -0.72]$, $\mathbf{N} = [0.80, 0.60, 0.07]$

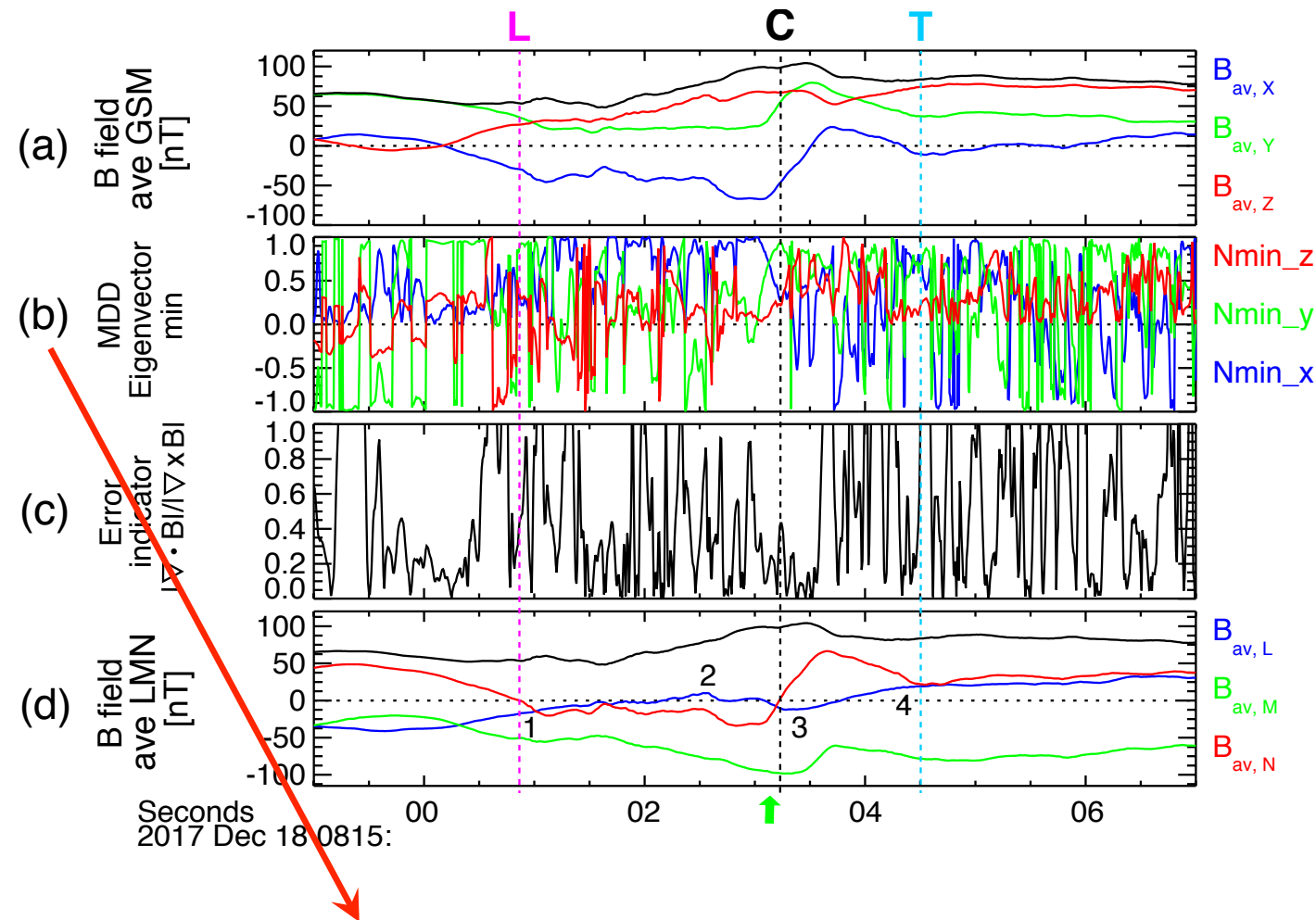
Using MTA, **duskward and southward propagation**: $[-0.99, 0.07, -0.14]$ in LMN
(consistent with the maximum shear model)

FTE cross-section (**L**-to-**T**) : $\sim 12.2 d_i$



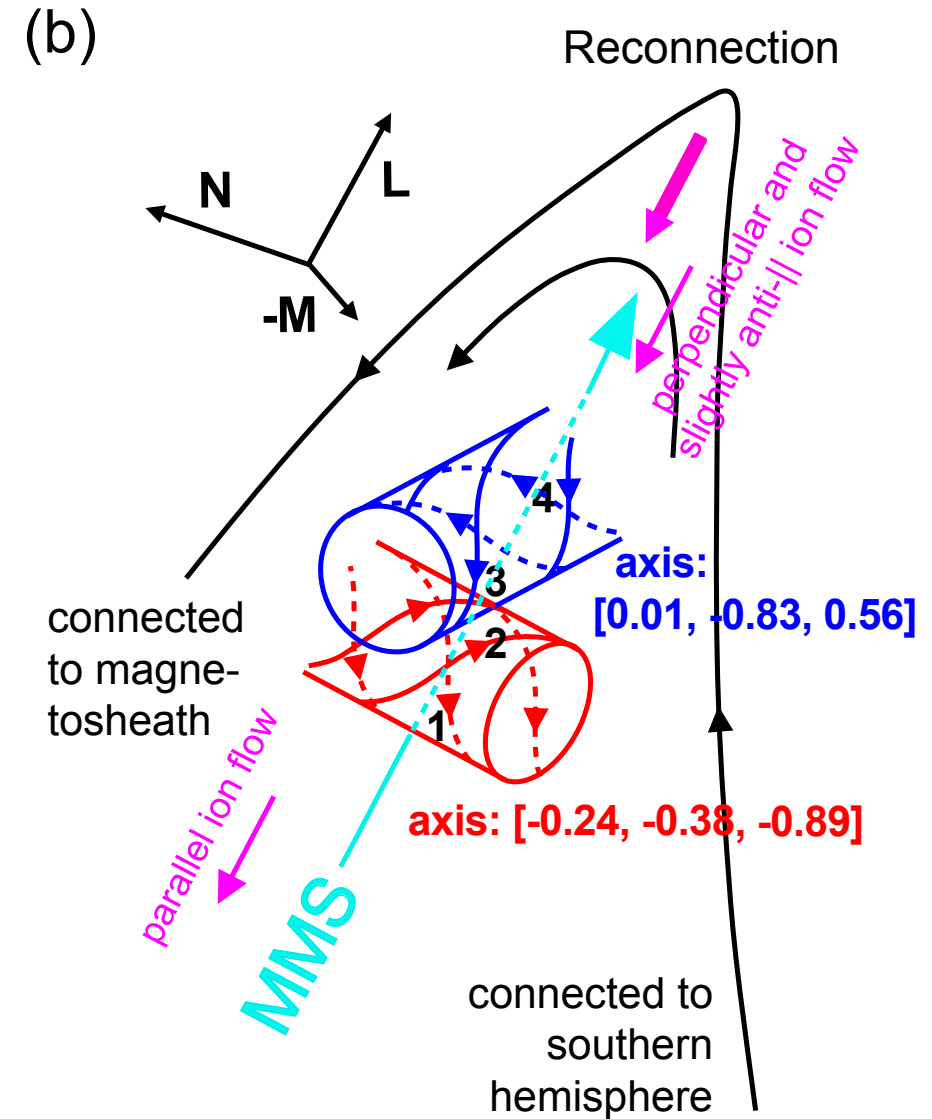
Prediction from maximum shear model:
White traces show primary X-lines. A component reconnection X-line is located dawnward and northward of the MMS location (blue rectangle), leading to a **duskward and southward motion of an FTE**

Evidences of two interlinked FTEs (1)



Minimum- λ eigenvector (FTE axis) from MDD (b):

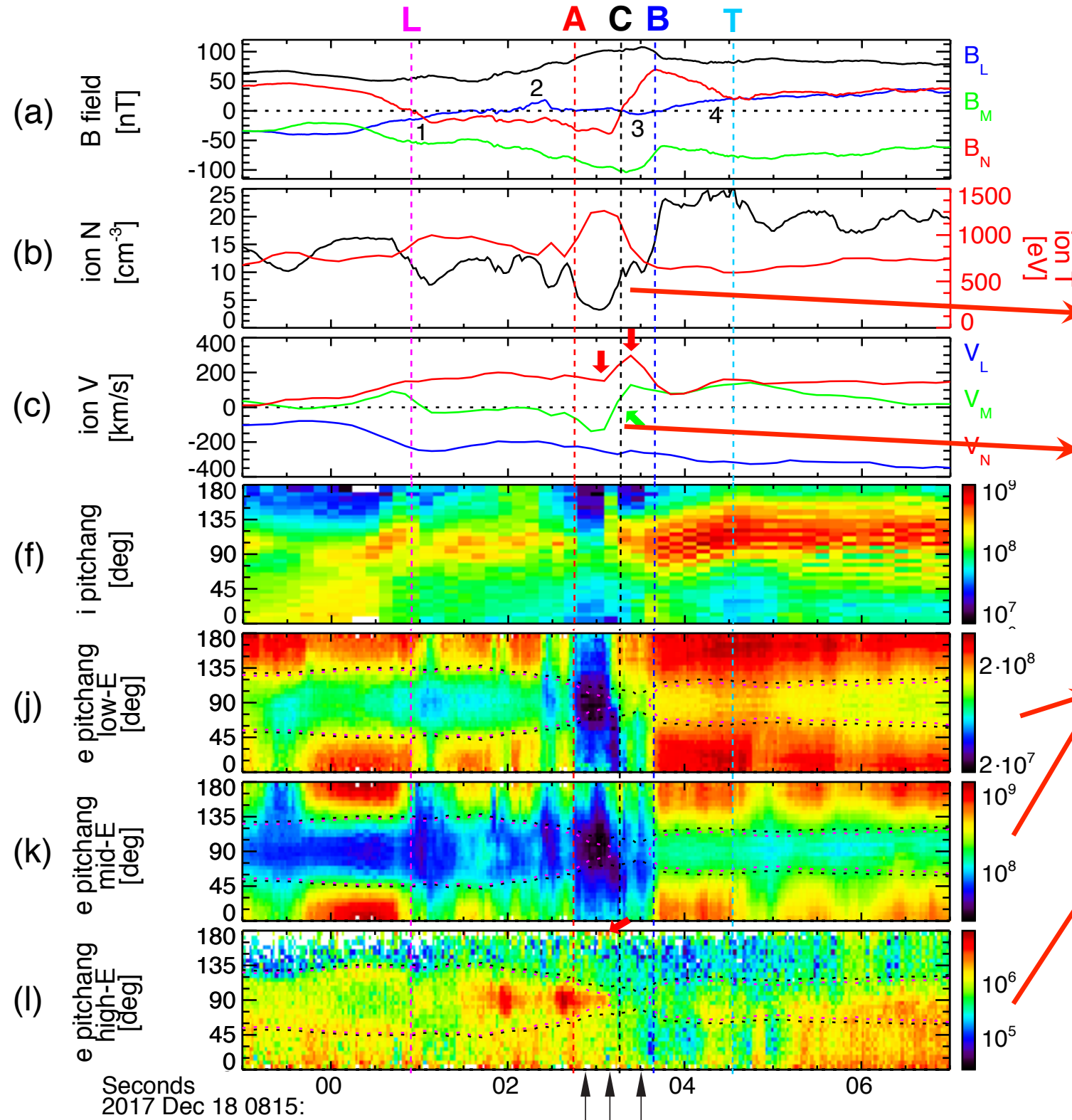
- ✓ L~C: mostly along x or $[-0.24, -0.38, -0.89]$ in LMN
- ✓ C~T: mostly in (y, z) or $[0.01, -0.83, 0.56]$ in LMN



The FTE structure when viewed mostly from the $-M$ direction. Note the **two flux tubes** that **oriented almost perpendicularly**.

Evidences of two interlinked FTEs (2)

A. MMS4 at [9.0, -1.2, 1,3] R_E



Plasma parameters show notable differences across 'C':

(b) ion density (temperature) is lower (higher) during L~C than C~T

(c) $V_{i,M}$ changes from - to + across 'C'

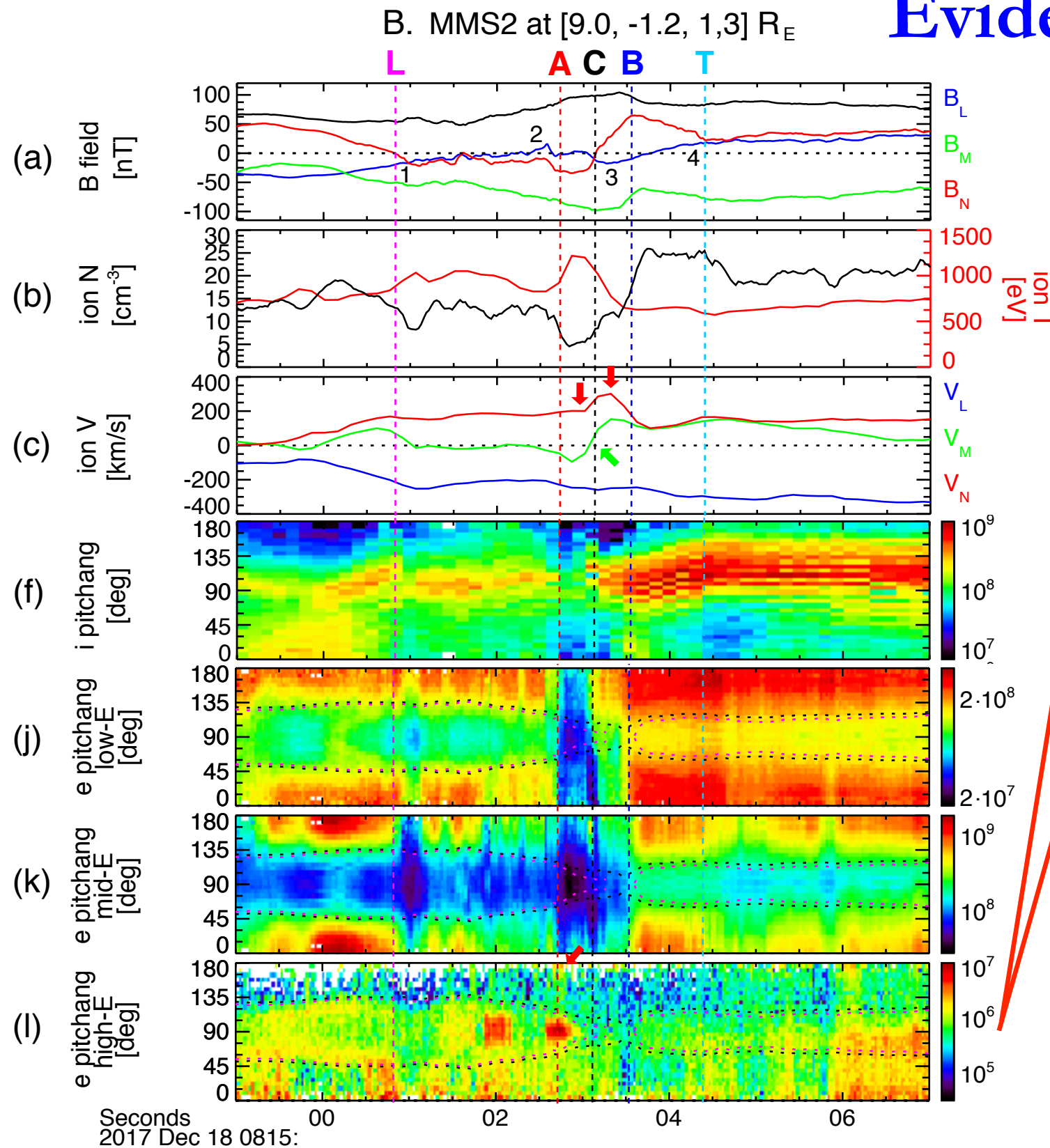
(j-k) Electron PAD exhibit dramatic changes across 'C':

✓ Low and mid energy electron fluxes (j, k) were lower between L~C than C~T

✓ 90° pitch-angle electrons enhanced in the high-energy range (l) only before 'C'

These significant differences in the electron PAD across the FTE center indicate two interlaced flux tubes [Kacem et al., 2018]

Evidences of two interlinked FTEs (3)

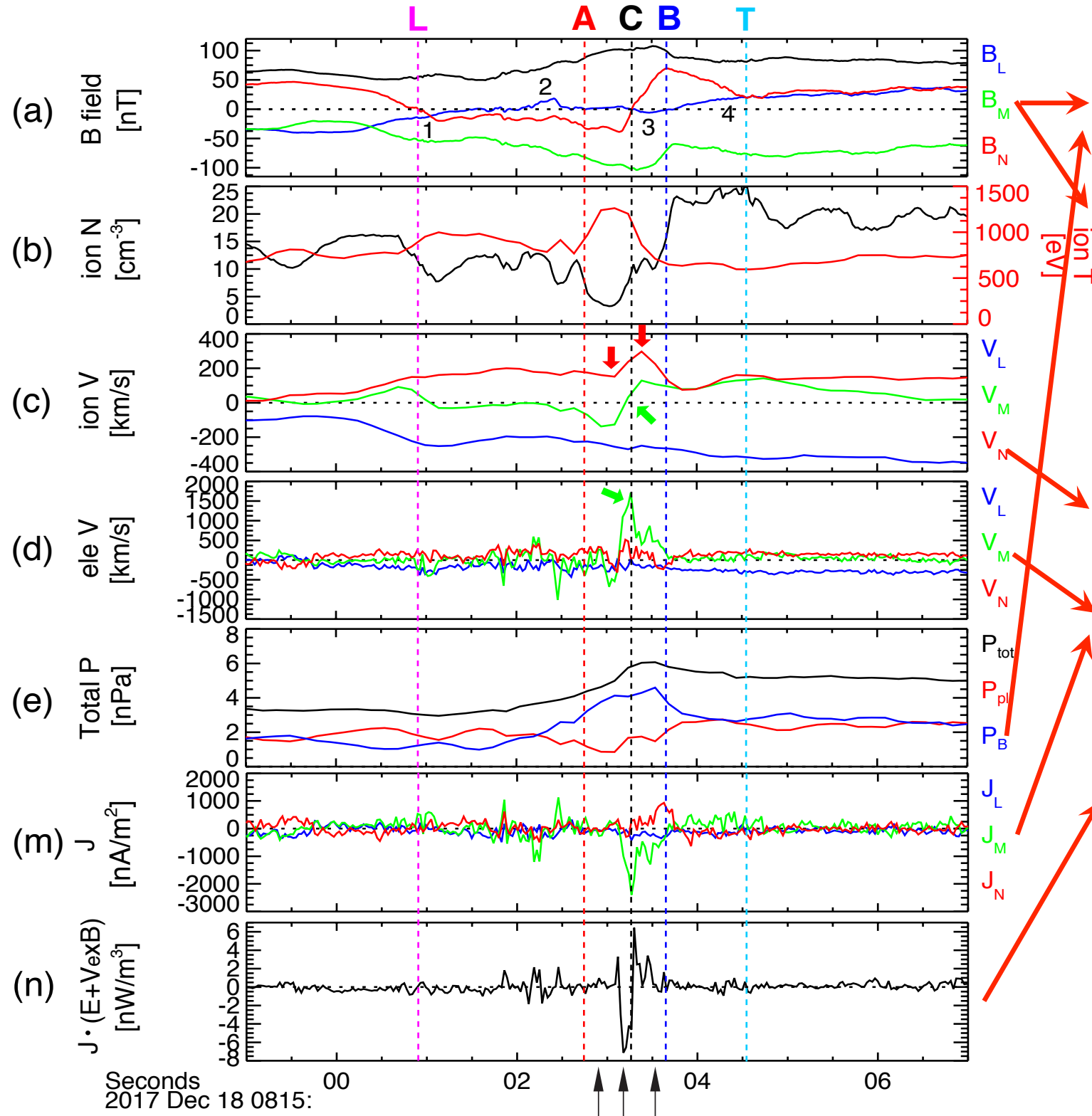


The intense 90°-focused energetic population is likely to be trapped on the field lines connected to both hemispheres (supported by the low density and high temperature of the plasma in b)

The absence or reduction of such high-energy populations between 'C' and 'T' indicates magnetosheath field lines or open field lines that allow hot magnetospheric populations to escape.

Completely different magnetic connectivity before and after the center of the FTE inferred from the electron PAD strongly supports the interpretation of two interlinked flux tubes, instead of a single flux-rope-type FTE.

Evidences for RX at the interface of two flux tubes (1)



(a, e) $|B|$ reduction/suppression at 'C' might result from local reconnection.

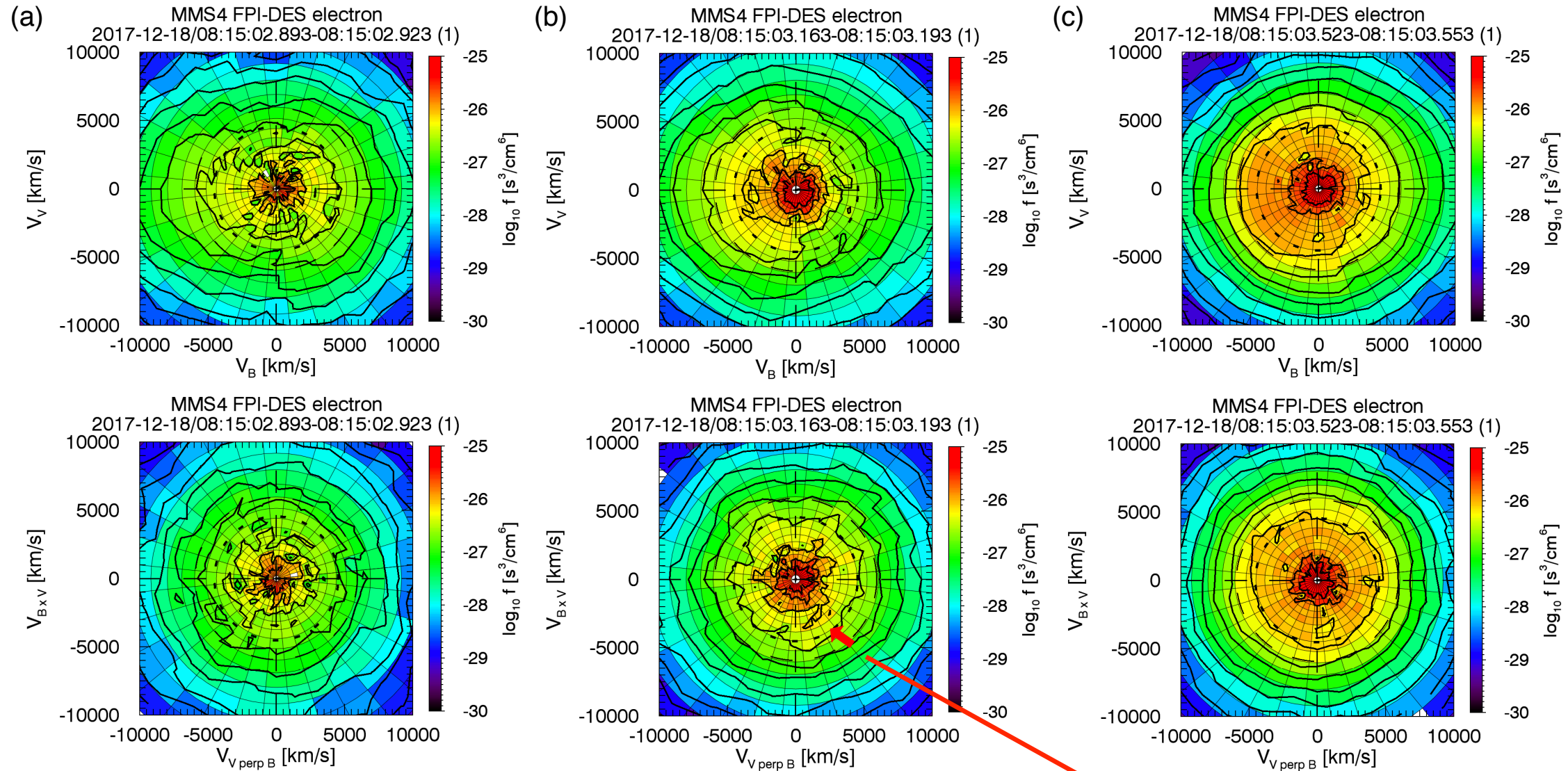
(a) An abrupt change in B_N , indicating a local current sheet (a). [Note that L , M , and N axes correspond to N , $-M$, and L axes, in nominal 2-D reconnection geometry]

(c) Ion outflow jets directed along N

(d) Out-of-plane electron jets along M carrying a significant electric current (m).

(n) $J \cdot E'$ fluctuated and showed negative values before/around 'C', indicating strong interactions between fields and plasmas with the negative values implying the outer edge of the electron diffusion region or associations with waves.

Evidences for RX at the interface of two flux tubes (2)



Electron distributions as a function of ($V_{||}$, $V_{\perp 1}$) (upper) & ($V_{\perp 1}$, $V_{\perp 2}$) (lower):

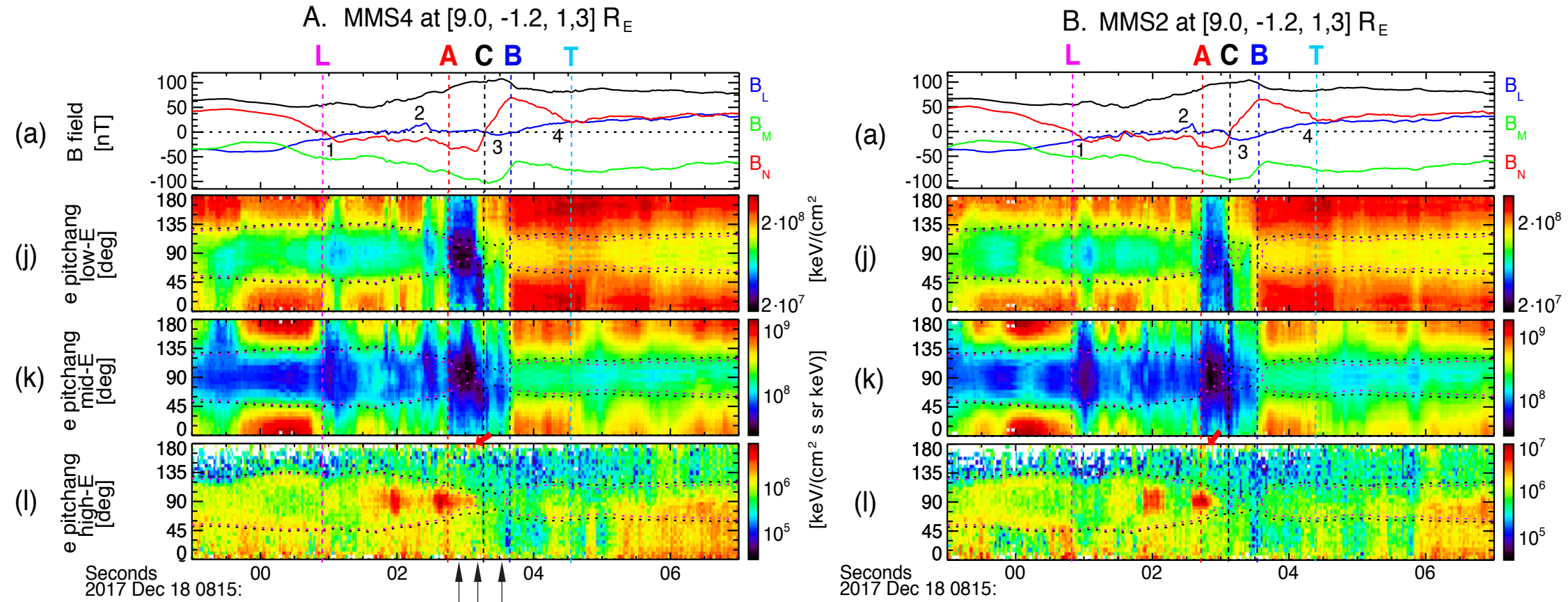
(a) A low-density, high-temperature magnetospheric electron distribution

(c) A heated, antiparallel-streaming magnetosheath electron distribution

(b) A mixture of the two populations

Note that the ($V_{\perp 1}$, $V_{\perp 2}$) distribution shows a certain level of agyrotropy (red arrow).

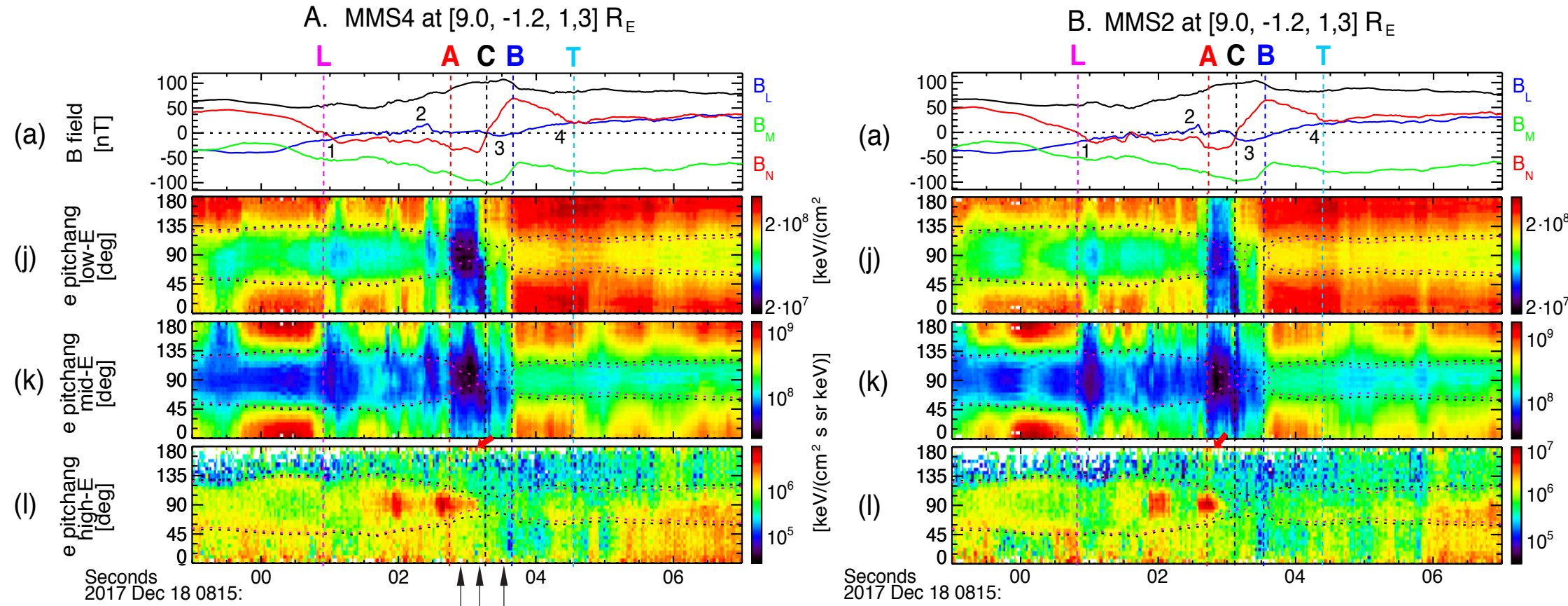
Magnetic topology of the interface of two flux tubes (1)



Dramatic changes in the electron PADs before and after ‘C’:

- ✓ A significant reduction in the low and mid energy electron fluxes (j, k) immediately before C, (A~L)
- ✓ These low (and mid) energy electrons were mostly counter-streaming during L~C, while low-energy electrons were mostly one-directional (anti-parallel) immediately after C during L~B.
- ✓ The **90° pitch-angle electrons were greatly enhanced** in the high-energy range (l) **only before C**.

Magnetic topology of the interface of two flux tubes (2)



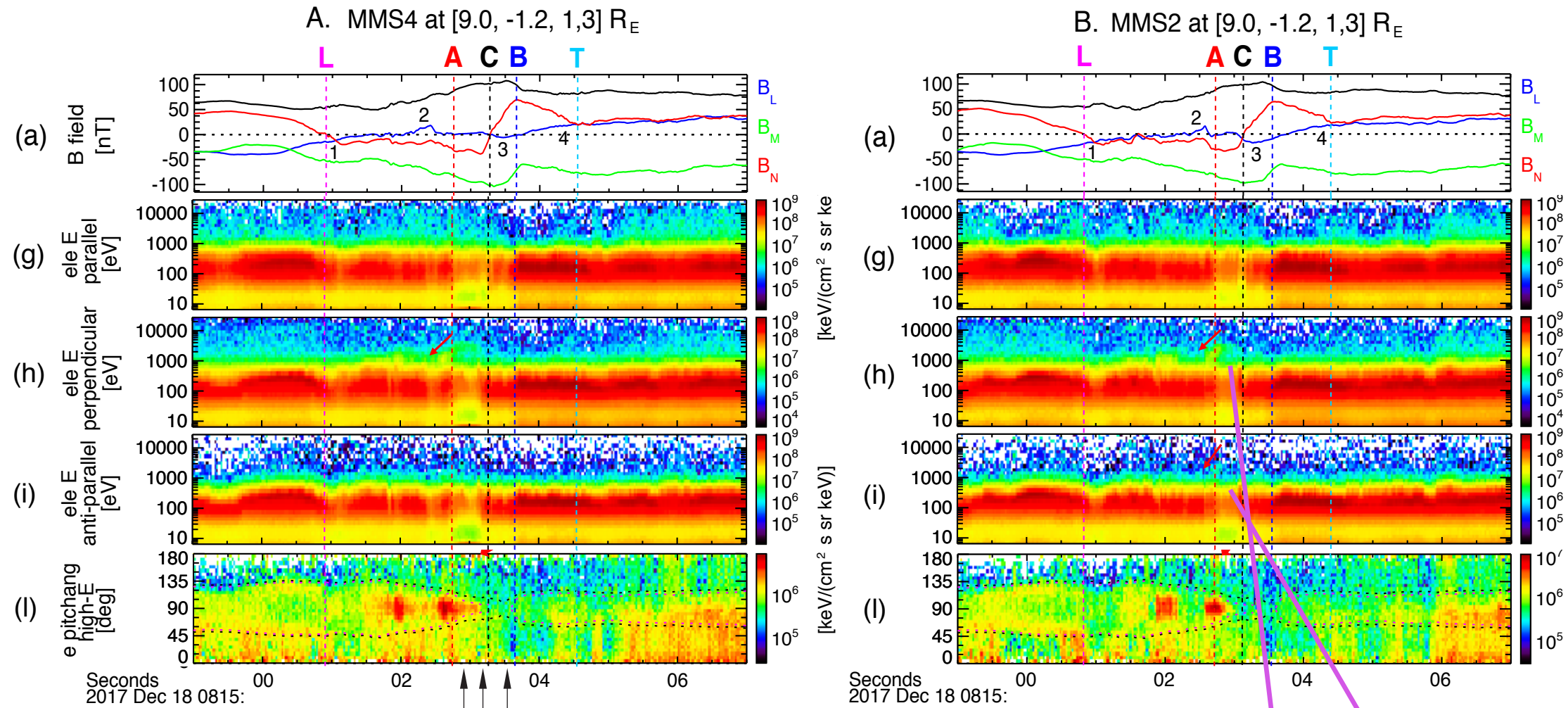
(j-l) black & magenta dotted contours represent loss-cone angles under an assumption that there is a mirror point with $|B|$ of 109 nT (black) or 100 nT (magenta).

90°-focused energetic electrons can be either **locally energized** or **trapped on the field lines connected to both hemispheres**:

- ✓ **The former** corresponds to trapped electrons locally bouncing within the exhaust region, showing a pitch-angle broadening at $|B|$ minima (dotted contours in j-l)
- ✓ **The locally bouncing/focusing population** will result in a **balance** in fluxes between **parallel** and **anti-parallel** components.

However, the **local energization cannot fully explain these 90°-focused energetic electrons** that were **exclusively observed before C**, and accompanied by the **imbalanced parallel and anti-parallel fluxes**.

Magnetic topology of the interface of two flux tubes (3)

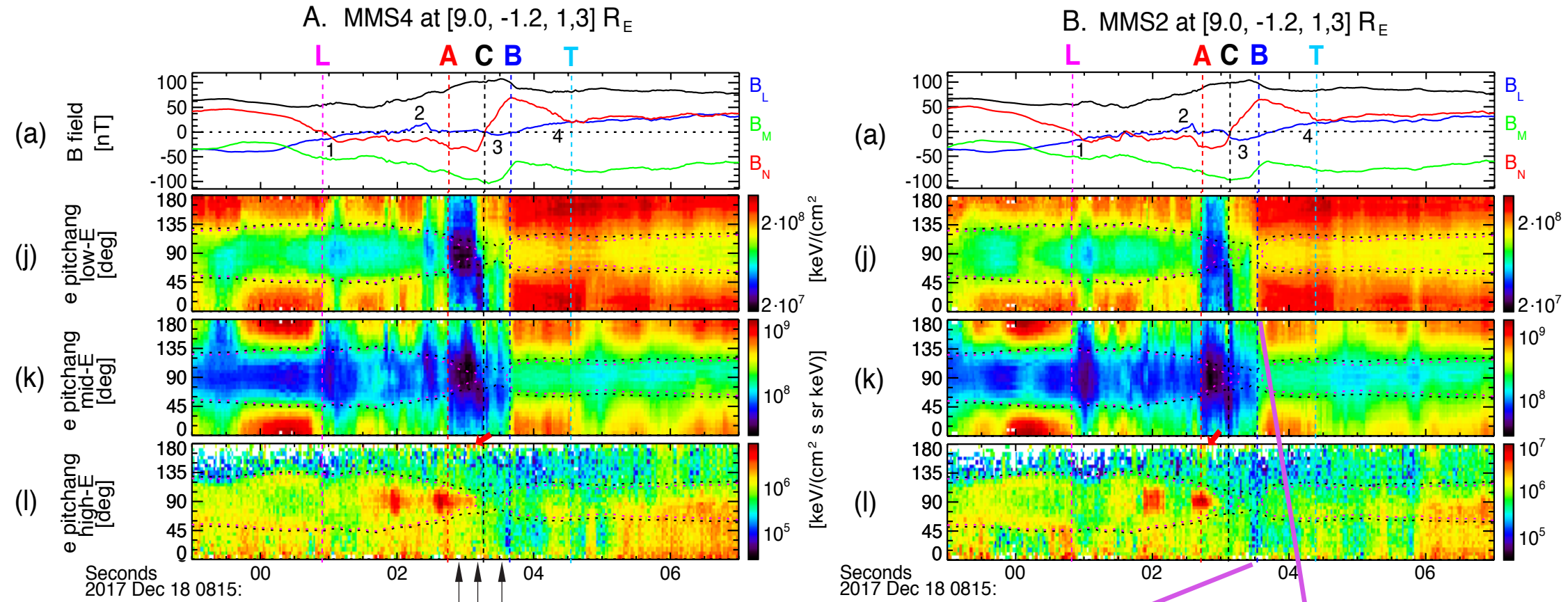


For **electrons being trapped on the field lines with their ends connected to both hemispheres**, it takes ~ 5 s (2 s) for 1 keV (10 keV) electrons to travel 5 R_E along the magnetopause field lines.

- ✓ The most energetic electrons on recently-closed field lines (via reconnection at the interface of the two flux tubes) will constitute the 90°-focused population, while less energetic electrons will lead to the imbalance between the parallel and anti-parallel fluxes.
- ✓ On the other hand, the most energetic electrons on early-closed field lines can escape away from the field lines, while less energetic ones remain trapped at 90°.

This feature is exactly seen as an inverse energy-time dispersion of high-energy electrons with perpendicular (or anti-parallel) pitch angles (red arrows in h and i).

Magnetic topology of the interface of two flux tubes (4)

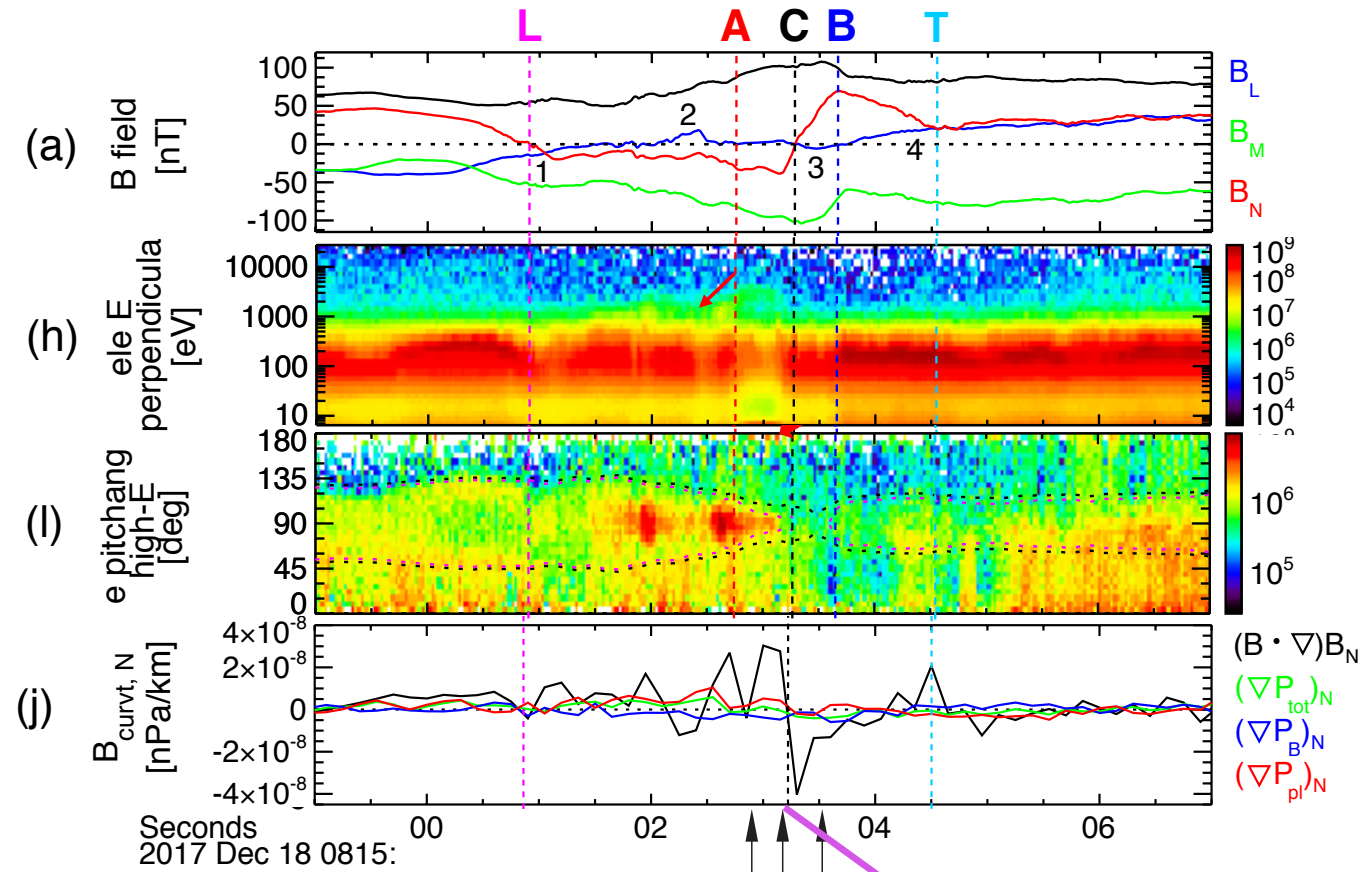


The absence or reduction of these 90°-focused energetic electrons after C' indicates magnetosheath field lines or open field lines with one end connected to the northern or southern hemisphere (l).

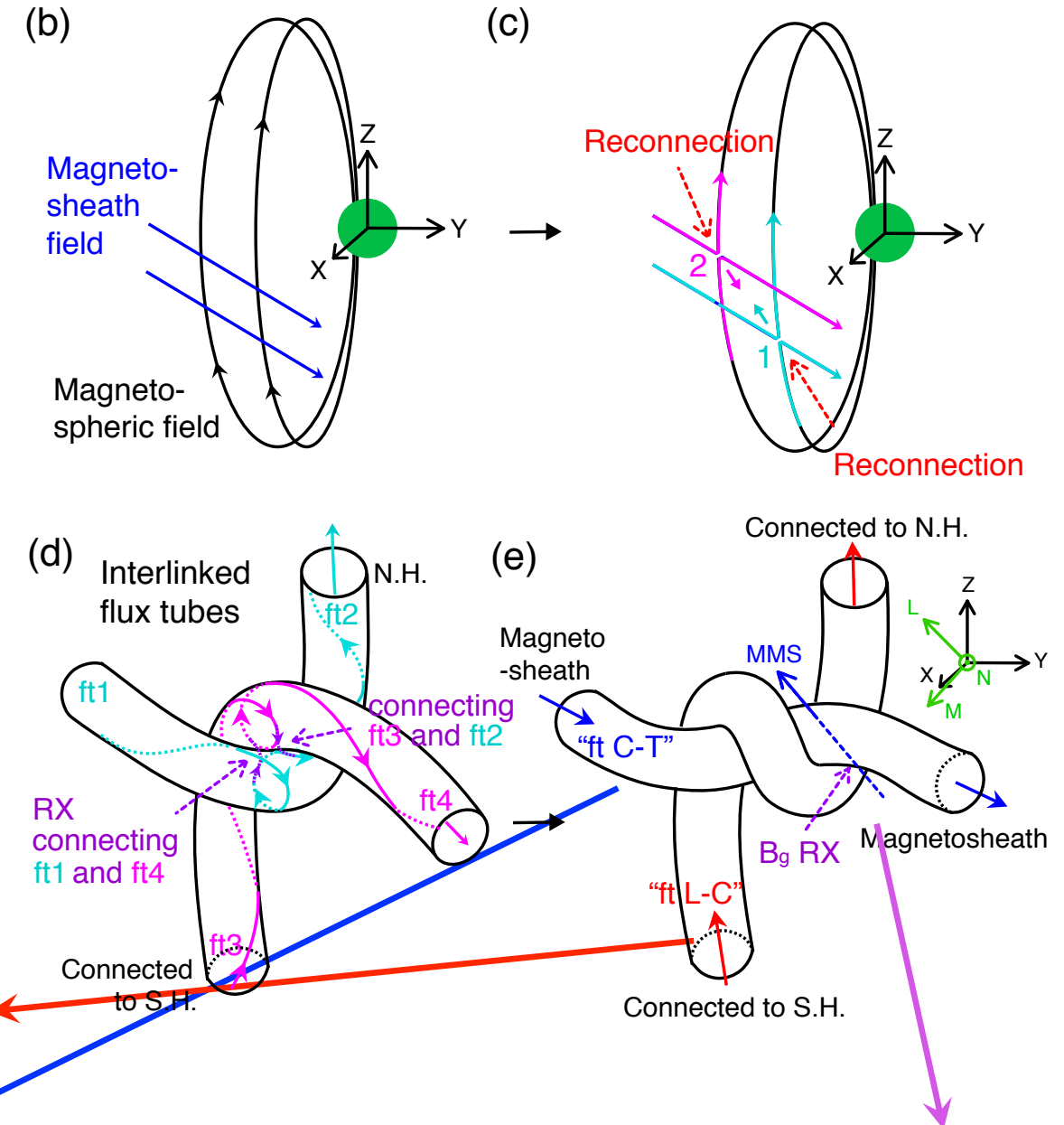
During C~T, the parallel high-energy population was still denser than the anti-parallel one, possibly due to the background effect associated with the FTE embedded in the southern exhaust region.

Before/around 'B', a notable reduction in these energetic electrons, together with uni/bi-directional low-energy electrons (j) indicates the magnetosheath field lines (with neither end connected to the hemisphere), on which the low-energy magnetosheath electrons flow along one direction or both directions with respect to B.

Magnetic topology of the interface of two flux tubes (5)

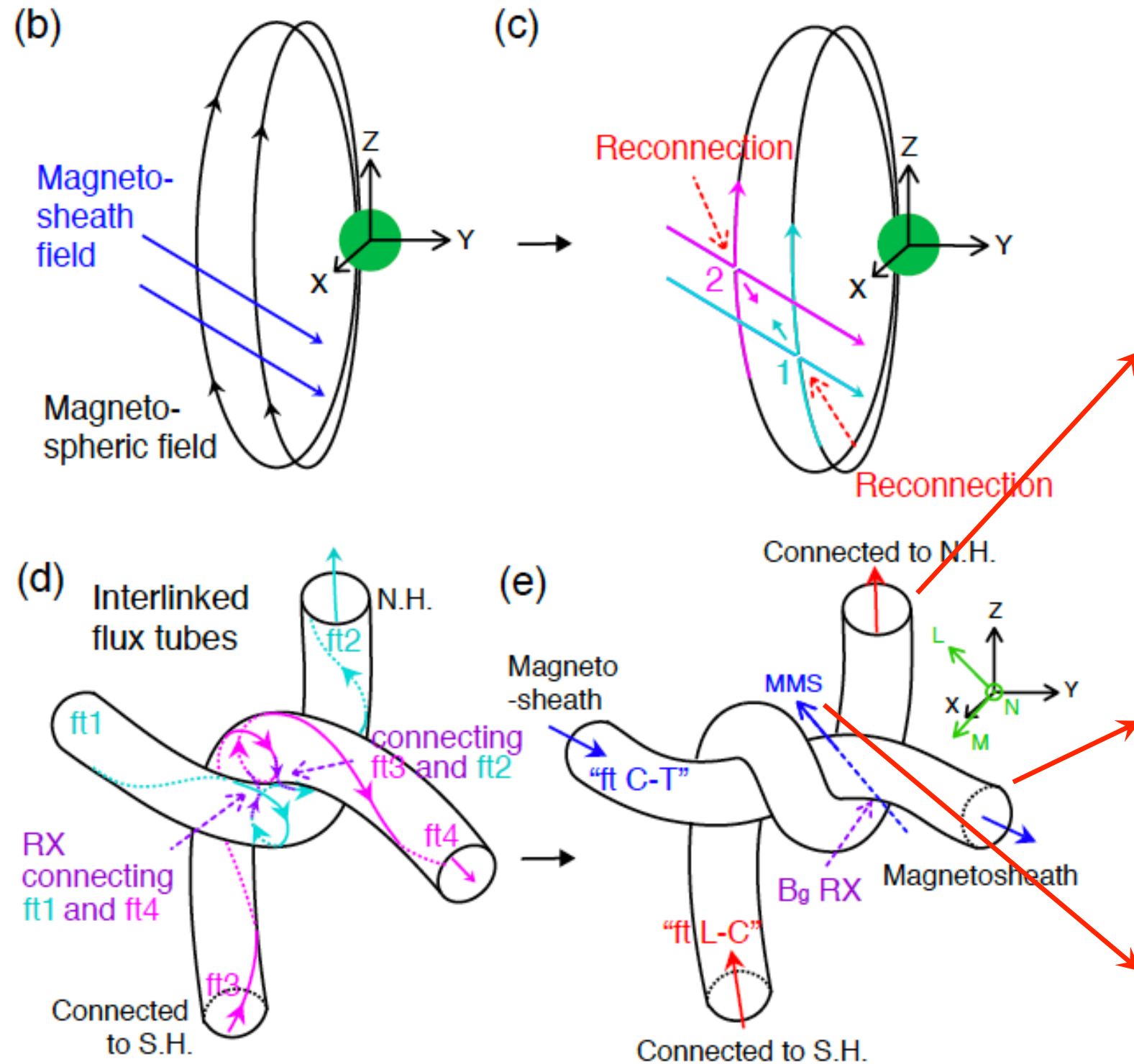


Thus, the **energy-dependent PAD variations across C** infer that the **two flux tubes** contain field lines of different magnetic topologies: **one with the field lines connected to both hemispheres** and **the other with open field lines connected to the magnetosheath** (further supported by the plasma density and temperature and particle distribution functions).



- The magnetic curvature, $(\mathbf{B} \cdot \nabla \mathbf{B})_N / \mu_0$ showing a clear, bipolar reversal from + to - across the interface

Conclusion (repeat): generation of interlinked flux tubes with their connectivity to either both hemispheres or the magnetosheath [Hwang et al., 2020; under review]



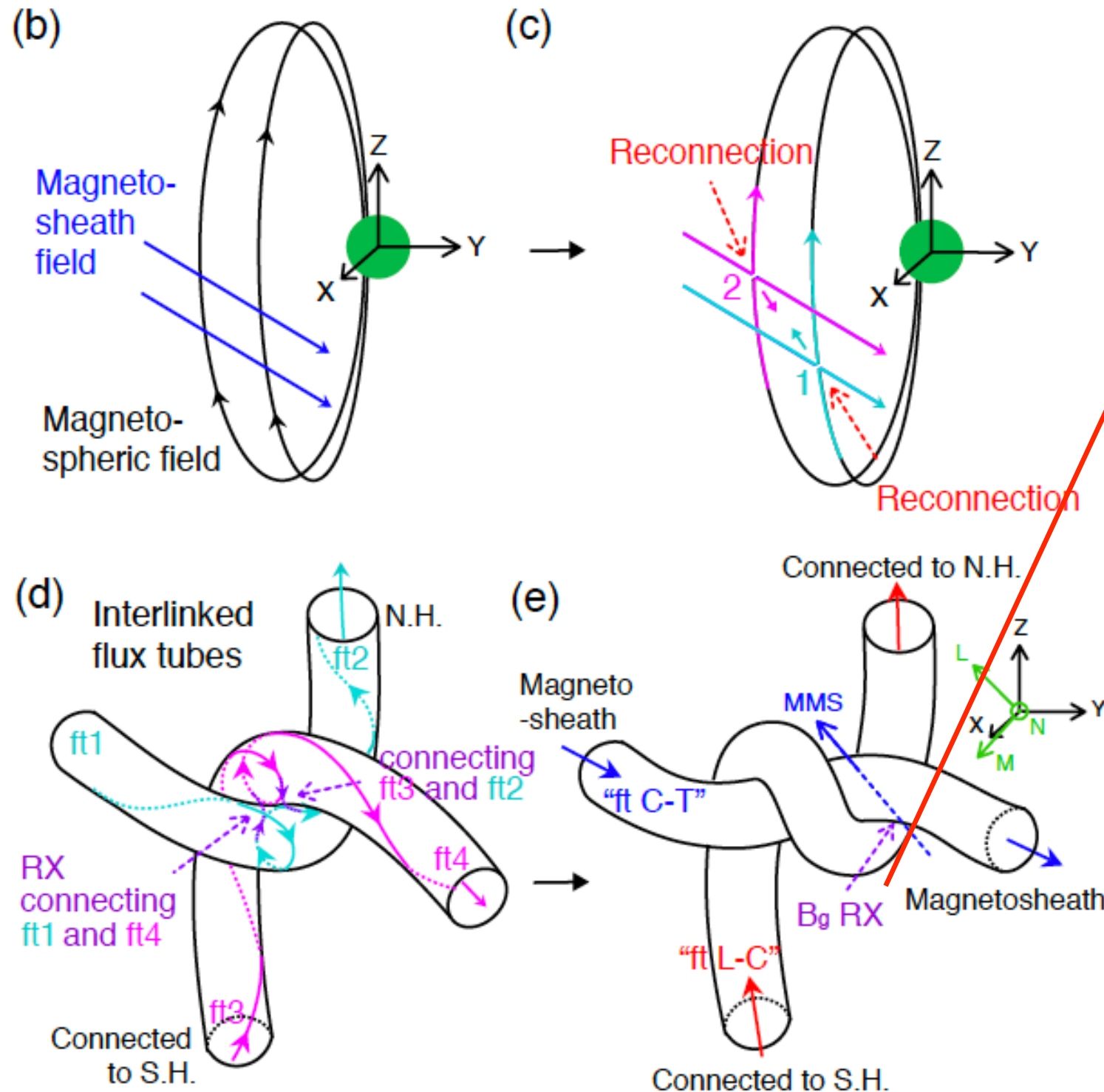
When the interface of the interlaced flux tubes undergoes reconnection (dashed violet arrows in d):

'ft1' and 'ft4' field lines are reconnected, constituting "ft C-T" with both ends connected to the magnetosheath (blue arrows in e).

'ft2' and 'ft3' field lines are reconnected, constituting "ft L-C" with both ends connected to the magnetosphere (red arrows in e).

MMS observed "ft L-C" first, then, "ft C-T"

Conclusion (repeat): generation of interlinked flux tubes with their connectivity to either both hemispheres or the magnetosheath [Hwang et al., 2020; under review]



Reconnecting flux tubes (d) result in a more complicated structure (e).

This structure exerts strong magnetic tension force toward the interface of the two interlinked flux tubes, which facilitates an interaction, i.e., reconnection of the interface (dashed violet arrows in e).

Evidences from MMS observations:

- **Perpendicular axes of two flux tubes**
- **Electron pitch angle distributions**
- **Reconnecting signatures at the interface.**
- **The magnetic curvature, $(\mathbf{B} \cdot \nabla \mathbf{B})_N / \mu_0$ showing a clear, bipolar reversal from + to - across the interface**

Conclusion and Indications

- Recent observations indicate that **local kinetic processes occurring within/around FTEs** play a **crucial role in the generation, structure, and evolution of FTEs**.
- The present event shows a new aspect of the **kinetic processes within FTEs** that lead to the **topological structure and evolution** of FTEs
 - A FTE consisted of two interlaced flux tubes
 - ✓ One flux tube included field lines **with both ends connected to the magnetosphere**
 - ✓ The other flux tube included **newly-opened magnetosheath field lines**.
 - Reconnection was undergoing at the interface of the two flux tubes
 - **This can lead to the formation of a large-scale flux rope, connecting both hemispheres**
 - **Potentially, this can regulate magnetic flux transfer** into the magnetosphere/magnetotail
 - ✓ When connected to both hemispheres, the flux tube becomes an efficient channel for solar wind transfer into the magnetosphere
 - ✓ The interlinking of flux tubes may suppress magnetic flux transfer into the magnetotail, via which FTEs can act for the main driver of the magnetospheric dynamics